

Device Characteristics of Nano Scale Junctionless Accumulation Mode FET (JAM-FET) with Localized Anti-channel Doping

Cheng-Li Lin^{1,a}, Jian-Dong Lee¹, Yao-Jen Lee², Yu-Jiun Lu¹, Wen-Kuan Yeh^{2,3}, Tsung-Kuei Kang¹, Pi-Chun Juan⁴, Yu-Zhang Zhu¹, and Tai-Yin Lin¹

¹Department of Electronic Engineering, Feng Chia University, No. 100, Wenhwa Rd., Seatwen, Taichung, Taiwan 407, R.O.C.

²National Nano Device Laboratories, Hsinchu 30010, Taiwan, R.O.C.

³Department of Electrical Engineering, National University of Kaohsiung, Kaohsiung 81148, Taiwan, R.O.C.

⁴Department of Materials Engineering, Mingchi University of Technology, Taipei, Taiwan 243, R.O.C.

Phone: +886-4-24517250 Ext. 4969

^aE-mail: clilin@fcu.edu.tw

1. Introduction

Traditional immersion mode (IM) MOSFET device requires sharp PN junction to achieve the source/drain region and to reduce the channel length variation [1]. When CMOS technology scaling down, the traditional IM MOSFET device requires the ultra-sharp (USH) source/drain (S/D) junction profile in channel region [2]. But the USH junction formation is difficult [2-4]. Recent years, devices without PN (or NP) S/D-channel junction have been used to overcome this issue, which is the junctionless FET (JLFET) or junctionless accumulation mode FET (JAM-FET) [5-7]. The JLFET presents the simple device process and more precise channel length [7-10]. Thus, the JLFET is one of the most promising candidates for the next generation of CMOS device application [11]. But, the JLFET is turned off by the depletion region in channel below the gate electrode. Using large work function difference between the gate and Si-channel to achieve the appropriate threshold voltage for JLFET [5]. In order to improve the I_{ON} current, the Si-channel requires high doping to increase the majority carriers and reduce the channel resistance. But this leads to increase the I_{OFF} current due to the small depletion region. In the other hand, reducing the channel doping could reduce the I_{OFF} , but the I_{ON} current is also decreased. Thus, optimum channel doping profile with large I_{ON}/I_{OFF} ratio and appropriate channel thickness are the key roles for the JLFET (JAM-FET) device design [12-15]. In this study, a localized anti-channel doping below the gate sidewall is proposed to improve the device characteristics of JAM-FET. Additionally, the n- and p-type JAM-FET devices w/ and w/o anti-channel doping are also compared and studied.

2. Experimental

A 6-in p-type Si wafer is used for the JAM-FETs fabrication. Firstly, the buried oxide (200 nm) and LPCVD Si_3N_4 (50 nm) were formed. Then, the amorphous Si (30 nm) was deposited and to form the Poly-Si channel by the solid phase crystallization (SPC). N- and p-type channel doping of phosphorus and BF_2 ions, respectively, with 1×10^{14} dose/cm² and the RTA process for the dopant activation. The active area was defined by the E-beam lithography and RIE etching. Then, the gate dielectric is the ALD Al_2O_3 (3.5 nm). The metal gate is PVD TiN (50 nm), and the gate area is defined by the 2nd E-beam lithography. The anti-ions-channel doping is formed by using the BF_2 and As ions of 2×10^{13} dose/cm² with a tilting angle of 45° to form the N⁻ and P⁻ regions below the gate sidewall for the n- and p-type JAM-FET devices, respectively. After spacer formation, a high same channel type doping was proceeded to form the S/D region. Finally, the PVD Al-Si-Cu metal (200 nm) was as the contact metal. The schematic of JAM-FETs and the detail process are shown in Fig. 1 and Fig. 2, respectively.

3. Results and Discussion

Fig. 3 and Fig. 4 show the $I_{DS}-V_{GS}$ curves of n- and p-type JAM-FETs, respectively, w/ and w/o anti-channel doping for W/L= 40/80 nm. The devices with anti-channel doping reveal the better performance, including the small I_{OFF} and large I_{ON}/I_{OFF} ratio for n- and p-type JAM-FETs. The I_{ON} is also decreased for device with anti-channel doping, but it is acceptance for the low power application. In addition, the p-type JAM-FET with anti-channel doping (Fig. 4b) reveals better characteristic than that of the n-type JAM-FET. From

the inset of the Fig. 3 and Fig. 4 related to the device performance of the subthreshold swing (SS) and the drain induced barrier lowering (DIBL), the anti-channel doping devices present the better characteristics. Fig. 5 and Fig. 6 show the $I_{DS}-V_{DS}$ curves of n- and p-type JAM-FETs, respectively, w/ and w/o anti-channel doping. For n-type device with anti-channel doping (Fig. 5b), the drain current is reduced and the I_{DS} curve presents the linear parasitic resistance behavior especially for the $V_{GS} > 1.2V$. This indicates the anti-channel doping below the gate sidewall destroy the origin channel doping profile in the bulk channel, resulting in the channel concentration decreased obviously. In addition, the p-type JAM-FET with anti-channel doping in Fig. 6b shows the smaller decrease of drain current (from 9.50 to 2.71 μA) than that of the n-type JAM-FET (from 3.85 to 0.526 μA), and there is smaller linear parasitic resistance behavior at large V_{GS} voltage (-2.0V). Presumably, the anti-channel doping ions (As) of p-type device is more weight than that of BF_2 ions of the n-type device, leading to the anti-channel doping did not implant deeper into the bulk channel and located near the surface below the gate sidewall. Thus, the P⁻ region is formed near the surface region of channel below the gate sidewall, resulting in the better $I_{DS}-V_{DS}$ performance. Fig. 7a shows the comparison of $I_{DS}-V_{GS}$ curves of n-type JAM-FET for the devices w/ and w/o anti-channel doping. There is larger reduction on I_{OFF} compared with the I_{ON} (reduced to 0.062 vs. 0.101 times). For the I_{ON} current of $I_{DS}-V_{DS}$ curve, the I_{ON} was decreased by 0.14 times (at $V_{GS}=2.0V$, $V_{DS}=2.5V$) compared with the device w/o anti-doping (Fig. 7b). In addition, the p-type device shows the smaller reduction of I_{OFF} and I_{ON} (reduced to 0.21 and 0.27 times, respectively) in Fig. 8a. The I_{ON} of $I_{DS}-V_{DS}$ is reduced to 0.42 times shown in Fig. 8b. In summary the p-type device reveals the better anti-channel doping process. Table I summarized the n- and p-type JAM-FET w/ and w/o anti-channel doping. The anti-channel doping can improve the SS, DIBL, and I_{ON}/I_{OFF} ratio, but the drain current is degraded.

4. Conclusions

The anti-channel doping near the gate sidewall will improve the performance of the SS, DIBL, and I_{ON}/I_{OFF} ratio. But the driving current will be degraded. Thus, the appropriate anti-ions concentration and the implanted energy are the important parameters to achieve the optimum device performance with good driving current.

Acknowledgements

This work was financially supported by the Ministry of Science and Technology (MOST), Taiwan, under Contract No. MOST 104-2221-E-035-049 and MOST 106-2221-E-035-089. We are also grateful to the National Nano Device Laboratory (NDL) providing the excellent process equipment for the device fabrication.

References

- [1] D.-Y. Jeon et al., *Solid-State Electronics*, 81, pp. 58-62, (2013).
- [2] C.-W. Lee, et al., *Solid-State Electronics*, 54, pp. 97-103, (2010).
- [3] M. S. Parihar et al., *Semiconductor Sci. & Tech.*, 29, 075006, (2014).
- [4] D. Hisamoto et al., *IEEE TED*, 47, pp. 2320-2325, (2000).
- [5] J.-P. Colinge et al., *Nature Nanotechnology*, 5, pp. 225-229, (2010).
- [6] C.-W. Lee et al., *Applied Physics Letters*, vol. 94, 053511, (2009).
- [7] S. Ramaswamy et al., *IEEE TED*, 63(11), 4185-4190, (2016).
- [8] M. H. R. Ansari et al., *IEEE TED*, 65(3), 1205-1210, (2018).
- [9] Jian-Dong Lee, *Master Thesis*, Feng Chia University, Taiwan, Feb., 2017.
- [10] C. L. Lin et al., *SSDM*, Sendai, 2017, pp.913-914.
- [11] H.-C. Lin et al., *IEEE TED*, 60, pp. 1142-1148, (2013).
- [12] S. K. Sharma et al., *IEEE Global Conf. Consum. Electron.*, 2015, pp. 556-559.
- [13] Y. Chen et al., *J. of Computational Electronics*, 12 (4), pp757-764, (2013).
- [14] L.-C Chen et al., *IEEE J. Electron Devices Soc.*, 4, pp. 50-54, (2016).
- [15] A. B. Sachid, et al., *IEEE EDL*, 37, 835-837, (2016).

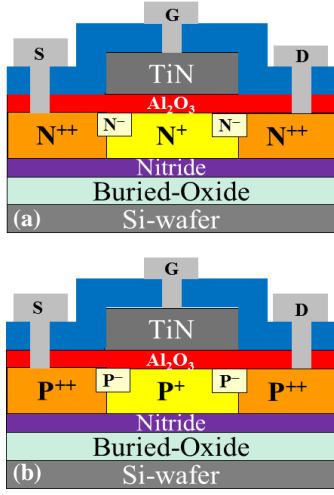


Fig.1 Schematic structures of (a) n-type and (b) p-type channel Junctionless accumulation mode FET (JAM-FET) transistors with anti-channel doping.

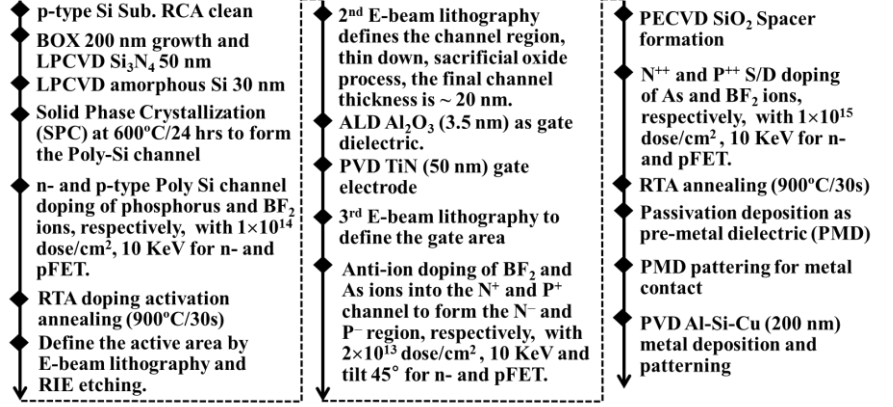


Fig.2 Fabrication process and deposition conditions for the n- and p-type Junctionless accumulation mode FETs with anti-channel doping. Without anti-channel doping JAM-FETs are also prepared for the comparison.

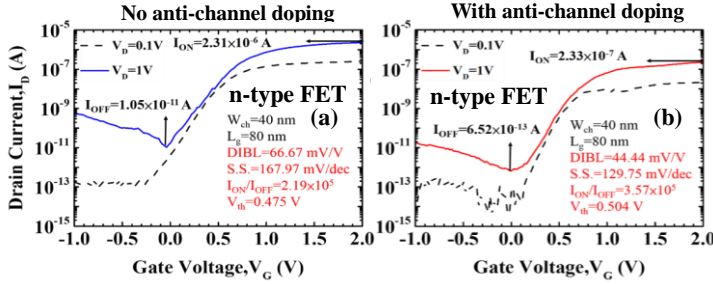


Fig.3 IDS-VGS curves of n-type JAM-FETs (a) without anti-channel doping, and (b) with anti-channel doping for the device dimension of W/L = 40/80 nm. The ION/IOFF ratio is calculated by the IDS-VGS curve at VDS=1.0V

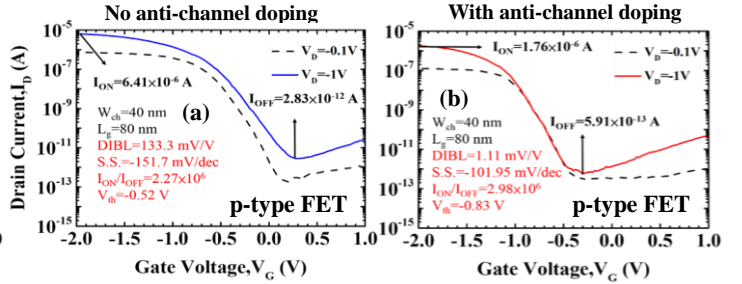


Fig.4 IDS-VGS curves of p-type JAM-FETs (a) without anti-channel doping, and (b) with anti-channel doping for the device dimension of W/L = 40/80 nm

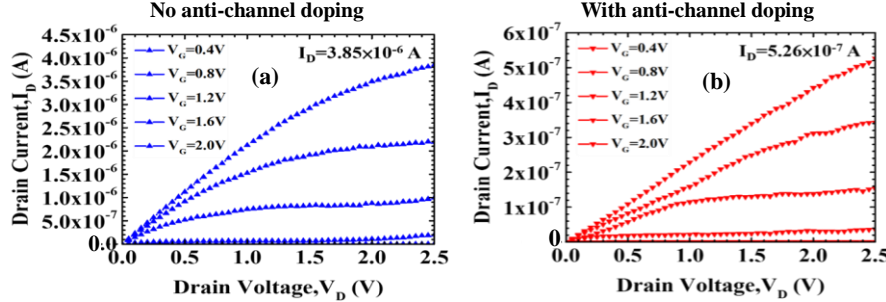


Fig.5 IDS-VDS characteristics of n-type JAM-FET (a) without and (b) with anti-channel doping for the device dimension of W/L = 40/80 nm.

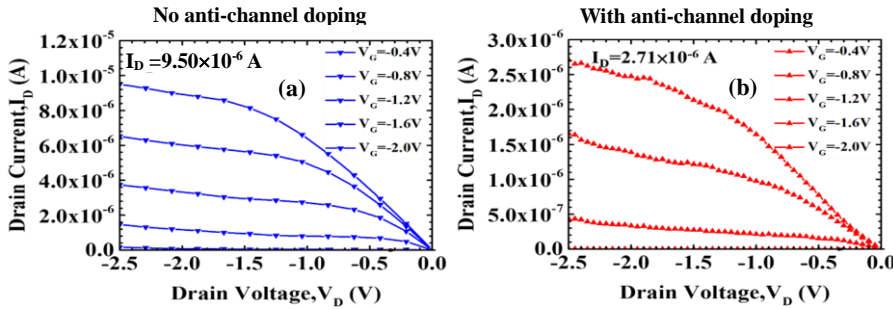


Fig.6 IDS-VDS characteristics of p-type JAM-FET (a) without and (b) with anti-channel doping for the device dimension of W/L = 40/80 nm.

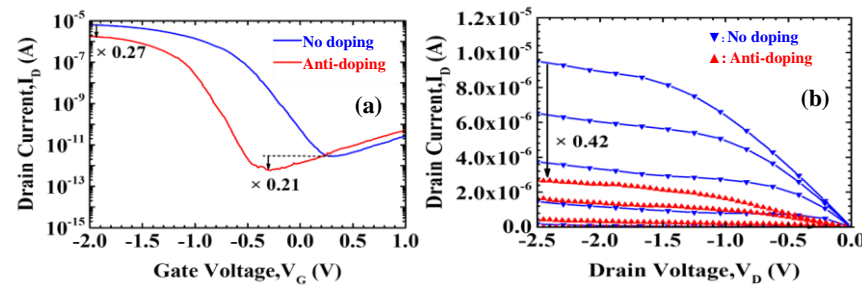


Fig.8 (a) IDS-VGS and (b) IDS-VDS characteristics of p-type JAM-FET with and without anti-channel doping for the device dimension of W/L = 40/80 nm.

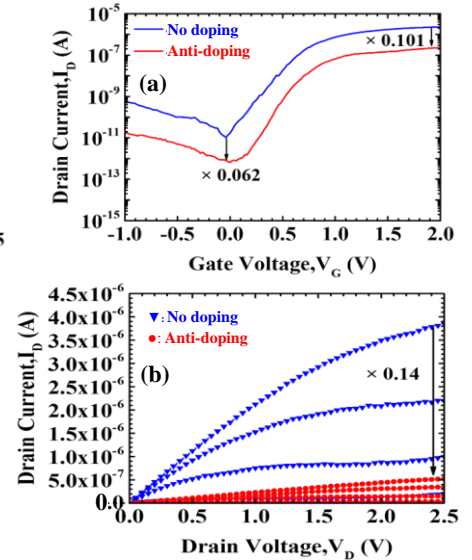


Fig.7 (a) IDS-VGS and (b) IDS-VDS characteristics of n-type JAM-FET with and without anti-channel doping for the device dimension of W/L = 40/80 nm.

Table I Device performance of n-type and p-type JAM-FET w/ and w/o anti-channel doping for W/L= 40/80 nm.

Device Performance	No doping	Anti-channel doping	No doping	Anti-channel doping
	n-type FET	n-type FET	p-type FET	p-type FET
SS (mV/dec)	167.97	129.75	-151.70	-101.95
DIBL (mV/V)	66.67	44.44	133.30	1.11
ION/IOFF ($\times 10^5$)	2.19	3.57	22.70	29.80
IDS,sat (μ A)	3.85	0.53	9.5	2.71
($ V_{GS} =2V, V_{DS} =2.5V$)				
Vth (V)	0.48	0.50	-0.52	-0.83